Catalysis Today 152 (2010) 24–32

Contents lists available at ScienceDirect

Catalysis Today

journal homepage: www.elsevier.com/locate/cattod

Desilication of ZSM-5 and ZSM-12 zeolites: Impact on textural, acidic and catalytic properties

Barbara Gil[a,*], Łukasz Mokrzycki[b], Bogdan Sulikowski[b], Zbigniew Olejniczak[c], Stanisław Walas[a]

[a] Faculty of Chemistry, Jagiellonian University, Ingardena 3, 30-060 Kraków, Poland
[b] Institute of Catalysis and Surface Chemistry, Niezapominajek 8, 30-239 Kraków, Poland
[c] Institute of Nuclear Physics, Radzikowskiego 152, 31-342 Kraków, Poland

ARTICLE INFO

Article history:
Available online 5 March 2010

Keywords:
Desilication
Acidity
ZSM-5 zeolite
ZSM-12 zeolite
α-Pinene isomerisation

ABSTRACT

Two zeolites of different topology: ZSM-5 and ZSM-12 were subjected to desilication in the NaOH solutions of increasing concentrations. Changes in the properties of modified zeolites were investigated by several methods (^{29}Si and ^{27}Al MAS NMR, FTIR, SEM, XRD, and sorption techniques). It was shown that desilication led to the formation of mesopores, and indicated that the process started at the faulting sites called "silanol nests" for ZSM-5 while this mechanism for ZSM-12 was different. Acidic properties of parent and desilicated zeolites were investigated by the adsorption of pyridine and CO followed by IR spectroscopy. For both zeolitic series the number of Brønsted acid centres was virtually independent of the desilication progress (differences below 20%), while the number of Lewis centres increased by more than 100% in some cases. Pyridine thermodesorption experiment revealed the presence of the second type of Brønsted sites in desilicated zeolites, their acidic properties may be compared to the hydroxyls existing in mesoporous materials of M41S family.

1. Introduction

Catalytic activity of zeolites is to the large extent controlled by the size and shape of their channels, which are of micropore dimensions. The presence of micropores, while advantageous for shape-selective reactions might impose diffusion limitations. Tailoring the porosity, hence diffusivity of zeolites, is one of the challenges in zeolite synthesis. Enormous synthetic effort to increase the size of channels resulted in successful synthesis of mesoporous materials with pores between 2 and 25 nm. Unfortunately, these mesoporous materials suffer from their low thermal stability and particularly from the absence of strong acid sites of Brønsted type.

Controlled mesopore formation for high-silica zeolites can be realized by the formation of hierarchical structures [1], cotemplating with mesoporous carbon [2] or desilication: extraction of the silicon from the framework by the treatment in basic solutions [3]. Some of the novel strategies for the development of micro/mesoporous composites were presented in the reviews of Van Donk et al. [4], Čejka and Mintova [5] or Mintova and Čejka [6].

Treatment with alkaline solutions might bring about various results, depending on the conditions used. In the case when aluminium source is available as extraframework species or added deliberately to a solution, realumination of the zeolite occurs [7,8].

Treatment with diluted bases in the absence of the additional aluminium source results in the ultimate removal of silica from the zeolitic framework, decreasing Si/Al ratio, and consequently increasing concentration of the acid centres present. Additionally, mesopores formation improves internal transport of bulkier molecules hence, in many cases, improving catalytic activity of the desilicated zeolite. It was shown that for high-silica zeolites in the intermediate Si/Al ratio, the formation of mesopores may be controllable [9].

Hierarchical zeolites may be also prepared via desilication by tetra-alkylammoniumhydroxide (TPAOH and TBAOH) solutions [10]. This method allows for avoiding an extra ion-exchange procedure, as subsequent calcination leads directly to the protonic form of zeolite. At the same time hierarchical structure may be achieved without the loss of the crystallinity [11]. Desilication may be also carried out in microwave-mediated conditions, accelerating the development of intracrystalline mesoporosity [12]. Among different zeolites, subjected to desilication ZSM-5 is the one, the most frequently used, but some other zeolite structures were also tested, e.g. ferrierites [13], beta [14] or mordenites [15]. Other framework trivalent heteroatoms can also regulate hydrolysis of silicon leading to the formation of the secondary mesoporosity [16].

The choice of α-pinene isomerisation as the test reaction was not accidental. First, the diameter of α-pinene (6.8 Å × 6.9 Å) [17] is significantly bigger than the diameters of the channels of both zeolites

* Corresponding author. Tel.: +48 12 663 20 16; fax: +48 12 634 05 15.
E-mail address: gil@chemia.uj.edu.pl (B. Gil).

0920-5861/$ – see front matter © 2010 Elsevier B.V. All rights reserved.
doi:10.1016/j.cattod.2010.01.059

Table 1
Structural features of zeolites under study.

Sample	Area, m^2/g			Volume, cm^3/g			Relative crystallinity degree, %
	Total	External	Micropore	Total	Micro-	Meso-	
ZSM-5	347	67	280	0.226	0.140	0.086	91
ZSM-5, 0.1 M	414	193	216	0.289	0.093	0.196	100
ZSM-5, 0.5 M	433	211	222	0.395	0.105	0.290	93
ZSM-5, 1.0 M	302	150	148	0.517	0.072	0.447	67
ZSM-12	342	103	239	0.479	0.100	0.379	90
ZSM-12, 0.1 M	294	125	169	0.240	0.081	0.159	100
ZSM-12, 0.5 M	306	167	139	0.421	0.072	0.349	81
ZSM-12, 1.0 M	280	189	91	0.578	0.043	0.535	43

chosen for modification; for ZSM-12: 5.6 Å × 6.0 Å and for ZSM-5: 5.3 Å × 5.6 Å at maximum. Thus, the reaction for the parent samples should be influenced to some extent by the restricted diffusivity of the substrate, which could be improved as a result of mesopores formation [14]. Secondly, the isomerisation of α-pinene proceeds on the acidic catalyst via confirmed formation of the carbenium ions not interacting with the Lewis acid centres [18]. Therefore, formation of Lewis centres, a known side-effect of the desilication reaction [19], would be possibly not influencing the course of the α-pinene isomerisation. The presence of basic sites leads to double-bond migrations, and thus formation of β-pinene [20]. The latter reaction was never observed in our case.

In the present work, two series of zeolites: ZSM-5 (Zeolyst) and ZSM-12 (home-made), both with the initial Si/Al ≈ 45, were desilicated using NaOH solutions of increasing concentrations at 85 °C.

2. Experimental

ZSM-12 zeolite was synthesized, following conditions given in Ref. [21], while ZSM-5 was provided by Zeolyst Inc. The initial Si/Al ratio of both zeolite samples was ca. 45. The materials were modified by desilication with 0.05, 0.1, 0.5 and 1.0 M NaOH solutions at 85 °C for 1 h, under atmospheric pressure. For each case, 25 ml of NaOH solution was heated up to 85 °C in a flask combined with reflux, then 3 g of the calcined (at 400 °C) zeolite was added and the mixture was vigorously stirred for 1 h. After modification, the zeolite samples were transformed into ammonium forms by fourfold ion exchange with 0.5 M ammonium nitrate (2 h) without calcinations in between ion-exchange procedures. Finally samples were transformed into the hydrogen forms by calcinations in vacuum at 550 °C. The parent and modified samples were characterized by ^{29}Si and ^{27}Al MAS NMR, FTIR, SEM, EDX, XRD, TPD and sorption techniques. Textural (XRD and SEM) properties of the samples were already described elsewhere [22].

The N_2 adsorption at 77 K was performed in a Quantachrome Nova 2000 series analyzer on samples activated in vacuum at 300 °C for 20 h. BET method was applied to calculate the total surface area, while discrimination between micro- and mesoporosity was done by the *t*-plot method.

Solid state Magic-Angle-Spinning Nuclear Magnetic Resonance (MAS-NMR) spectra were acquired on the APOLLO console (Tecmag) at the magnetic field of 7.05 T (Magnex). For the ^{29}Si MAS-NMR spectra a 3 μs rf pulse ($\pi/2$ flipping angle) was used, 4 kHz spinning speed, and 256 scans with the delay of 20 s were acquired. The ^{27}Al spectra were recorded using the 2 μs rf pulse ($\pi/6$ flipping angle), 8 kHz spinning speed, and 1000 scans with acquisition delay 1 s.

Catalytic tests (α-pinene isomerisation) were carried out in the liquid phase at 75 and 90 °C, using batch type reactors under reflux. For each run 5 ml of α-pinene was heated to chosen temperature. Subsequently, 250 mg of the catalyst (previously calcined to obtain the H-form) was added to the reaction mixture. Reaction was carried out under isothermal conditions with continuous stirring. After selected times (5, 15, 30, 60, 120 and 180 min) 12 μl of aliquots were obtained for analysis (ca. 2% of volume change). The reaction products were analyzed by GC (HP 5890) equipped with a packed column and a TCD detector.

Si and Al contents in the samples were determined in ICP AES study with the use of the Optima 2100 spectrometer (PerkinElmer, USA). RSD of determination were in the range of 0.18–2.22% for Al, and 0.13–1.86% for Si, respectively. Additionally, EDX analysis was recorded on a JEOL JSM 7500F electron microscope.

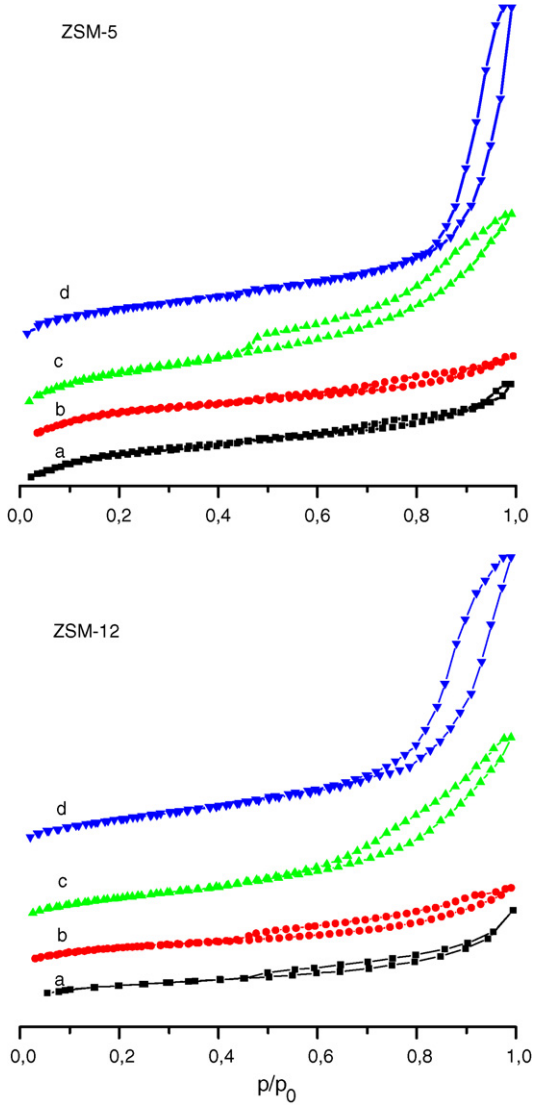

Fig. 1. Adsorption isotherms of the parent and desilicated ZSM-5 and ZSM-12 zeolites. a – non-treated zeolite, b – desilicated in 0.1 M NaOH, c – desilicated in 0.5 M NaOH, d – desilicated in 1.0 M NaOH.

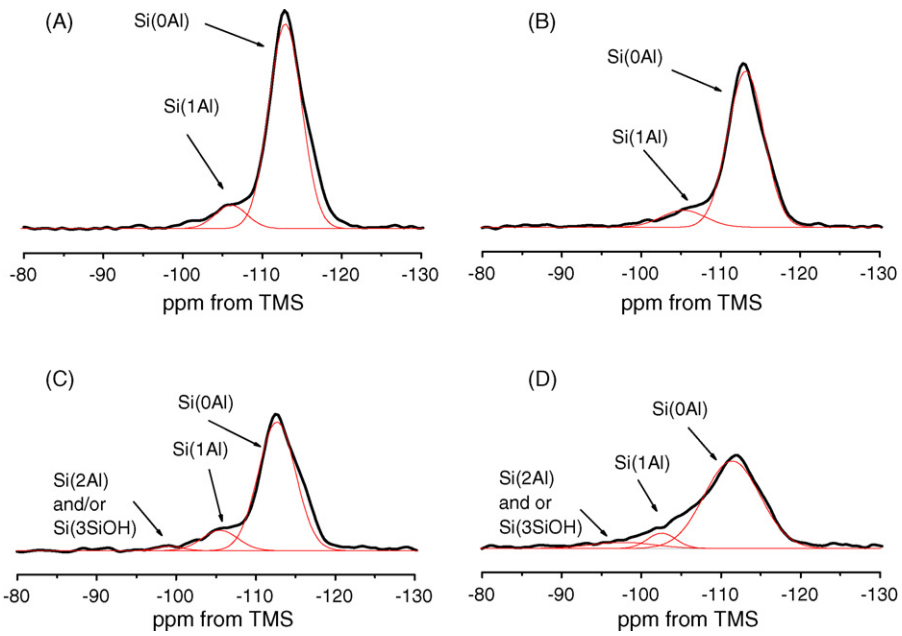

Fig. 2. ^{29}Si MAS NMR spectra of parent and desilicated zeolites ZSM-5. A – non-treated zeolite, B – desilicated in 0.1 M NaOH, C – desilicated in 0.5 M NaOH, D – desilicated in 1.0 M NaOH.

The acidity of zeolites was investigated by the adsorption of CO, pyridine and α-pinene used as probe molecules, followed by FTIR spectroscopy. All samples were activated in the form of self-supporting wafers (ca. 5 mg cm^{-2}) at 550 °C under vacuum for 1 h prior to the adsorption of probe molecules. The adsorption temperatures were: carbon monoxide at −100 °C, pyridine at 170 °C, and α-pinene at 75 °C. Spectra were recorded on a Bruker Tensor 27 spectrometer, equipped with an MCT detector, working at 2 cm^{-1} resolution. All measured spectra were recalculated to a 'normalized' wafer of 10 mg (density 3.2 g cm^{-2}). For quantitative characterization of acid sites the following bands and absorption coefficients were used: pyridine PyH$^+$ band at 1545 cm^{-1}, ε = 0.078 cm μmol^{-1} PyL band at 1454 cm^{-1}, ε = 0.165 cm μmol^{-1}.

3. Results and discussion

3.1. XRD studies

XRD measurements confirmed that the zeolite structure was preserved at lower NaOH concentrations, while the relative crystallinity (compared to the most crystalline samples of the series) of the samples treated by 1.0 M NaOH dropped to the level of ca. 70% (ZSM-5) and 40% (ZSM-12), see Table 1. These data suggest that

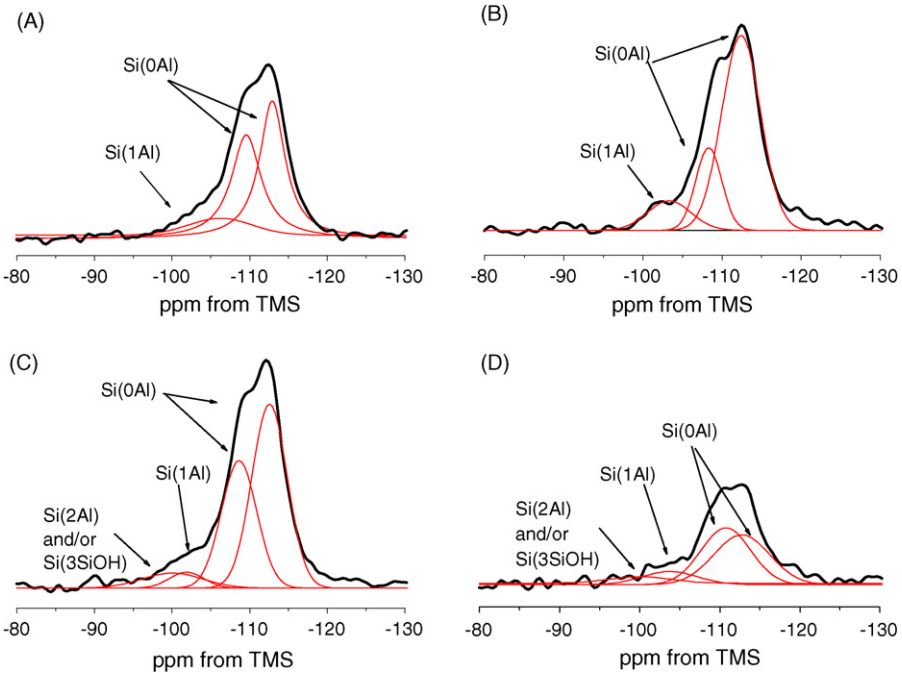

Fig. 3. ^{29}Si MAS NMR spectra of parent and desilicated zeolites ZSM-12. A – non-treated zeolite, B – desilicated in 0.1 M NaOH, C – desilicated in 0.5 M NaOH, D – desilicated in 1.0 M NaOH.

the MFI structure of ZSM-5 zeolite is more resistant to destructive force of NaOH that the MTW structure of ZSM-12 of the same Si/Al ratio. Two facts have to be emphasized at this point. Firstly, the most crystalline samples for both series are the one treated with 0.1 M NaOH which suggest that the parent zeolites already contain some extraframework amorphous phase, very easily removed in basic solution. Secondly, the presence of the amorphous part must influence the results of the acidity measurement. All the results are calculated for the 'normalized' weight of the catalyst and one have to be conscious of the fact that some part of this weight is made up by crystalline and some of the amorphous phase. At the same time the catalytic results are calculated also for the catalyst weight therefore the 'diluting' effect of the amorphous phase is influencing the acidity and activity measurement to a similar extent.

3.2. N_2 adsorption studies

Desilication caused changes in the pore structure, as showed by the N_2 sorption experiments, the isotherms are presented in Fig. 1. For both zeolites, the increase in the external surface area was accompanied by the significant increase of the mesopore volume and decrease in the micropores area. At the same time, the total sample surface area after modification did not change considerably. Such behaviour can be explained by the formation of mesopores at the expense of micropores. It can be assumed that the part of the micropores may be blocked by the extraframework material. Removal of silicon atoms with accompanying oxygen atoms may result in the formation of silica-rich, amorphous debris. The extent of formation of such extraframework material was rather limited for desilication in NaOH of concentrations up to 0.5 M since it was observed that crystallinity of the corresponding samples was only slightly changed (Table 1). This hypothesis will be further confirmed by the NMR and IR studies (*vide infra*).

3.3. NMR studies

^{29}Si MAS NMR spectra (normalized to the mass of the samples, Figs. 2 and 3) show three, poorly separated peaks located between −105 and −112 ppm, which can be assigned to Si(0Al), Si(1Al) sites, and one, common for Si(2Al) and SiOH sites. From the relative intensities of these peaks some information about the desilication can be deduced: whether it is completely random process, or if there is a preferential removal of Si atoms near neighbouring Al atoms. The signal characteristic of Si(0Al) is dominating the spectra both for the parent and modified samples, and its relative intensity is gradually decreasing with the desilication progress. An increase of the relative intensity of the signal at −105 ppm is caused more by the increase of the number of SiOH groups (confirmed by IR, *vide infra*), than by the increase of the number of Si(2Al) sites. The latter possibility can easily be rejected from consideration after noticing that the intensity of Si(1Al) signal is decreasing as well, which can be best observed for the ZSM-12 series (Fig. 3). If the abundance of Si(1Al) groups does not increase during desilication, the abundance of Si(2Al) groups should not increase either, as seen by the deconvolution results. Furthermore, the OH groups connected with Si(1Al) or Si(2Al) sites should display slightly different acidic character, caused by the so-called chemical factor [23], thus the number of the next-neighbouring Al atoms, decreasing the partial charge located on the acidic proton. Changes in acidity can be easily followed by IR spectroscopy and will be presented later.

Since NMR spectroscopy can be considered as quantitative method, from the intensities of the Si signals in the ^{29}Si MAS NMR spectra the values of Si/Al were calculated, according to the method presented in Ref. [24] after deconvolution into separate signals (Figs. 2 and 3). The results are presented in Table 2 together with the ICP and EDX analysis results. Si/Al ratios are systematically lower when calculated on the basis of the NMR and EDX than from ICP, reflecting partial amorphization of the desilicated material.

Table 2
Si/Al ratio, calculated from ICP AES analysis, ^{29}Si MAS NMR spectroscopy and the concentration of the Brønsted and Lewis acid sites (IR spectroscopy on the basis of pyridine adsorption).

Sample	Si/Al			Concentration, μmol/g		
	ICP	NMR	EDX	Brønsted		Lewis
				Strong	Weak	
ZSM-5	49.6	39.7	48.2	256	49	60
ZSM-5, 0.1 M	47.8	34.1	43.2	197	54	28
ZSM-5, 0.5 M	37.1	23.7	–	179	86	31
ZSM-5, 1.0 M	18.9	18.5	18.1	211	112	148
ZSM-12	47.0	41.5	21.1	193	18	38
ZSM-12, 0.1 M	44.1	34.7	44.4	188	54	57
ZSM-12, 0.5 M	43.2	21.1	30.3	157	94	110
ZSM-12, 1.0 M	32.1	17.7	15.6	130	126	166

^{27}Al MAS NMR spectra (Fig. 4) are dominated by the signal at 60 ppm, originating from tetrahedral aluminium sites, while the number of the octahedral species (signal at 0 ppm) is small. Nevertheless, for both series, the intensity of the signal at 0 ppm is gradually increasing with desilication, suggesting progressive damage of the zeolitic framework (amorphization).

From the analysis of the NMR spectra it can be concluded that there seem to be no preference in the way Si (or Al) atoms are removed from the framework. Only small increase of the intensity

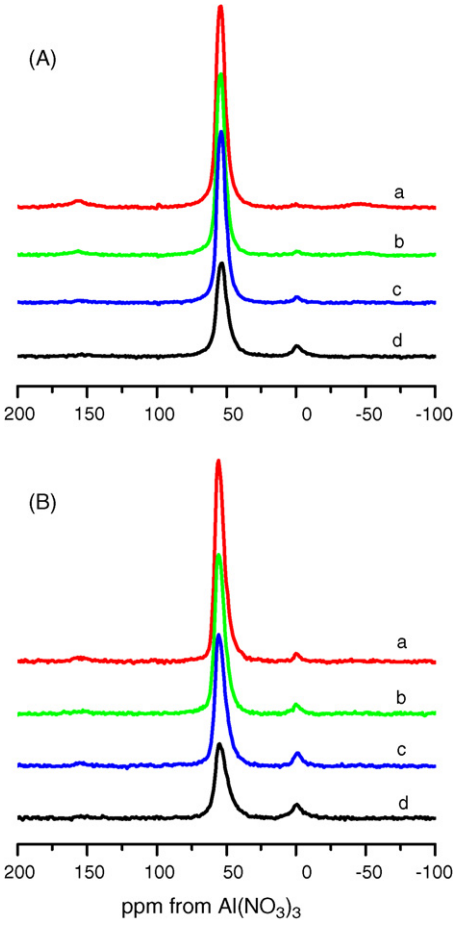

Fig. 4. ^{27}Al MAS NMR spectra of parent and desilicated zeolites ZSM-5 (A) and ZSM-12 (B). a – non-treated zeolite, b – desilicated in 0.1 M NaOH, c – desilicated in 0.5 M NaOH, d – desilicated in 1.0 M NaOH.

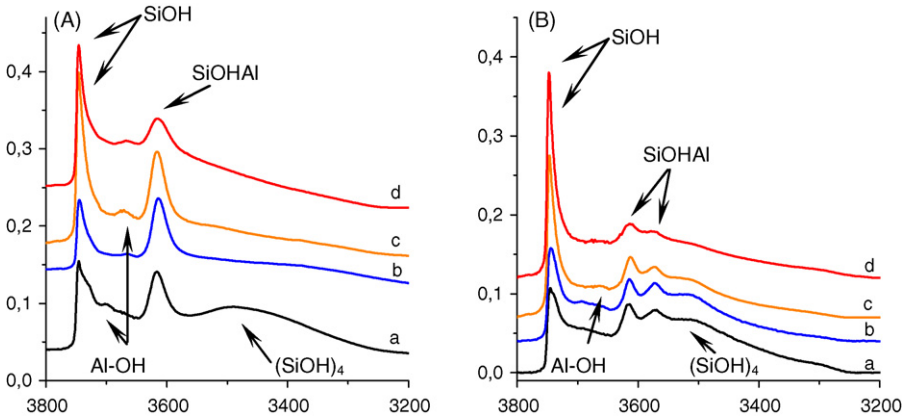

Fig. 5. IR spectra in the OH region for parent and desilicated zeolites ZSM-5 (A) and ZSM-12 (B), where a – non-treated zeolite, b – desilicated in 0.1 M NaOH, c – desilicated in 0.5 M NaOH, d – desilicated in 1.0 M NaOH.

of the octahedral Al signal suggest that extraframework material is rather washed away than remaining and blocking internal pores.

3.4. IR studies of the OH groups

Changes in the structure of desilicated zeolites can be followed by IR spectroscopy, exploring the distribution of different kinds of OH groups in the first place. Fig. 5 presents the spectra of the parent and desilicated zeolites ZSM-5 and ZSM-12 normalized to the same sample density (3.2 g cm^{-2}). It can be observed that due to desilication defect sites, known as the "silanol nests" were removed in the first order. The IR band characteristic for these groupings (at 3500 cm^{-1}) in zeolite ZSM-5 decreased its intensity after reaction with 0.1 M NaOH and disappeared almost completely after treatment with 0.5 M NaOH (Fig. 5A). It can be deduced that these defect sites are the places the most incurred to the attack of the base. Such suggestion was very recently proposed by Holm et al. [19]. For zeolite ZSM-12 the band characteristic for silanol nests is steadily decreasing with increased base concentration, but is visible even after treatment with 1.0 M NaOH (Fig. 5B, spectrum d), suggesting slightly different desilication mechanism. Differences may arise from different T-site density of both zeolites and different dimensionality of the channel system: three-dimensional for ZSM-5 and one-dimensional for ZSM-12. Differences in the internal transport may play a role in a removal of dissolved fragments of the framework, bearing in mind similar channel dimensions and Si/Al ratio of both zeolites.

For zeolite ZSM-5 in the spectrum of non-treated sample, the band at 3700 cm^{-1} is present. This band corresponds to the OH groups, attached to the extraframework aluminium species, which are the most probably located on the external surfaces of the crystals [25]. Treatment in even diluted base solutions readily removes these defects. On the contrary, the extraframework aluminium species of other character is formed as a result of desilication, with the characteristic band at 3670 cm^{-1}. Both for ZSM-5 and ZSM-12 zeolites, the band at 3670 cm^{-1} appears when the concentration of NaOH reaches 0.5 M. Analogous in the frequency and shape band is observed of ZSM-5 zeolites with low Si/Al ratio and is characteristic for OH groups attached to intrachannel, extraframework Al species [26]. The appearance of the band at 3670 cm^{-1} is accompanied by the decrease of the intensities of bands, characteristic

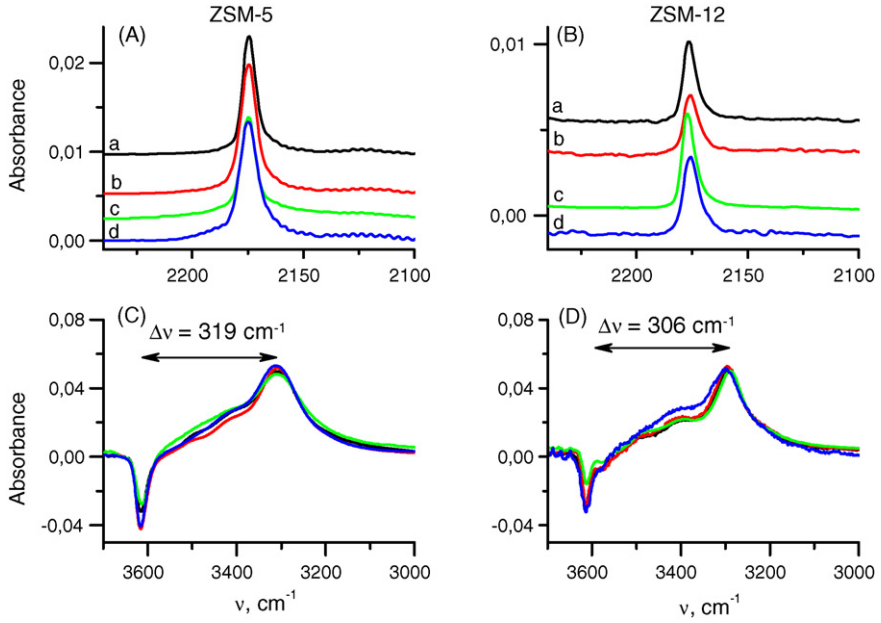

Fig. 6. IR spectra of CO, adsorbed on parent and desilicated zeolites. Spectra in the region of CO stretching vibrations (A and B) and of OH groups interacting with CO (C and D). Spectra on parts C and D are subtraction spectra, resulting from the subtraction of spectra of activated sample from the spectra after CO adsorption and normalization to the same intensity of the OH···CO band. a – non-treated zeolite, b – desilicated in 0.1 M NaOH, c – desilicated in 0.5 M NaOH, d – desilicated in 1.0 M NaOH.

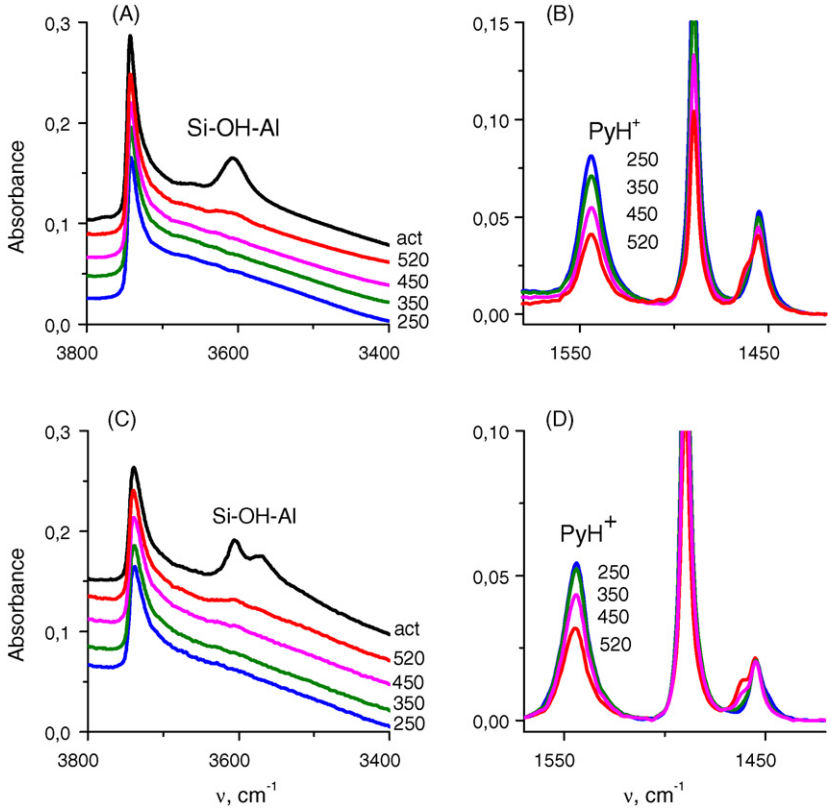

Fig. 7. IR spectra of OH groups (A and C) and PyH^+ (B and D) on zeolite ZSM-5 (A and B) and ZSM-12 (C and D), recorded during pyridine desorption at 250, 350, 450 and 520 °C. Spectra in C and D are the subtraction spectra (spectrum after Py desorption minus spectrum of activated zeolite).

for Si–OH–Al groups. Treatment with NaOH seems to decrease the number of acidic OH groups with increased concentration of the base. This observation confirms the results from NMR measurement, which suggest removal of both Si and Al atoms from the zeolite framework. Formation of the mesopores is connected with the increase in the intensity of SiOH groups with the band at 3745 cm^{-1}. Silanols, with such high stretching frequency, are the so-called terminal silanols, located almost exclusively on the external surfaces of zeolite crystals. The mesopores' surface can be considered as the external, with its 'chemistry' closer to the mesoporous silica than microporous zeolite.

From the analysis of the IR spectra of OH groups alone it can be concluded that the treatment with NaOH caused increase in the amount of external silanol groups, now located mostly in the mesopores, and dealumination of the samples, manifested in the decrease of the intensity of Si–OH–Al groups together with the appearance of extraframework Al-oxo/hydroxo species.

3.5. IR studies of CO sorption

Carbon monoxide, when adsorbed on acidic zeolites can distinguish between Brønsted and Lewis sites. Furthermore, differentiation between Lewis sites, appearing in the zeolite as a result of dehydroxylation (IR bands at 2230 cm^{-1}) from the 'intrinsic' Lewis sites [27] analogous to the ones present in Al_2O_3 (IR band at 2180 cm^{-1}) is also possible. This differentiation is feasible only when using CO as a probe molecule. Pyridine and ammonia 'recognize' both types of Lewis sites as one. Unfortunately, the frequency at which the band of adsorbed CO appears is not a direct measure of the strength of the Lewis site [28]. CO interacts with Lewis acid centres in the first order, and only after that it starts to interact with OH groups. The band of CO bonded onto Brønsted sites at 2175 cm^{-1} is so intense that it would obscure much less intense bands of CO–Lewis complexes. Fig. 6A and B shows therefore the spectra of the small amount of CO (ca. 2–3 molecules for a unit cell) adsorbed in zeolites. For both series of zeolites, the band characteristic of Lewis sites originating from dehydroxylation is absent. Slight broadening (appearance of the tail on the higher frequency side) of the band at 2175 cm^{-1}, observed for desilicated zeolites (Fig. 6A and B, spectra b–d) may be a result of the appearance of the band at 2180 cm^{-1}, so the presence of the intrinsic Lewis acid sites. It has to be noted that the intensities of CO–Lewis complexes are very small due to extremely low absorption coefficient of this band, thus on the basis of the intensity of this band it would be extremely hard to judge the amount of the Lewis sites. This was done in the experiment with pyridine adsorption, and taking into account the absence of the Lewis acid sites originating from dehydroxylation, only the 'intrinsic' Lewis sites are present in both series of zeolites.

The interaction between CO and OH groups is frequently used to estimate the acid strength of the Brønsted sites. Carbon monoxide was introduced into the contact with zeolites at −100 °C in the amount enabling interaction with all OH groups present. When CO is adsorbed on acidic OH groups, the O–H bond is weakened and corresponding stretching frequency shifted towards lower frequencies (red-shifted). At the same time, the intensity of such band is lowered and half-width increased. The bigger the value of the frequency shift the more acidic are interacting OH groups. Additionally, as the perturbed band is wider the differences in the acid strength which may be caused by desilication, should be much easier to observe. The value of the red-shift for ZSM-5 is equal to 319 cm^{-1} and 306 cm^{-1} for ZSM-12 (Fig. 6C and D) pointing at the slightly higher acid strength of OH groups in zeolite ZSM-5. Subsequently recorded spectra were subtracted from the spectra of activated samples and normalized to the band at ca. 3500 cm^{-1} (Fig. 6C and D). For both series of zeolites, the shape of the red-

shifted band is not changing with the desilication progress; this concerns both the value of the red-shift ($\Delta\nu$) and the half-width of the band of interacting OH groups. Therefore it can be concluded that the acid strength of the Si–OH–Al groups is not influenced by desilication.

3.6. IR studies of pyridine sorption

Adsorption of pyridine, followed by IR spectroscopy allows quantification of the acid sites, both Brønsted and Lewis types.

Excess pyridine was adsorbed in zeolites at 170 °C, subsequently desorbed for 20 min at high vacuum (residual pressure 10^{-4} mbar) at 170, 250, 350, 450 and 520 °C. After desorption at the desired temperature, the sample was cooled down to 170 °C and the IR spectrum recorded to rule out the influence of the temperature on the intensity and the half-width of the IR maxima.

The experiment preformed in this manner allowed establishing two aspects of acidity. The first is the concentration of Brønsted and Lewis centres, determined from the intensity and the absorption coefficients of the 1545 cm^{-1} band of protonated pyridine (Brønsted sites) and the 1450 cm^{-1} band of coordinatively bonded pyridine (Lewis sites). The second is the relative acid strength determined under dynamic conditions. Desorption of pyridine, having kinetic diameter 5 Å, from the microporous channels of the parent zeolites of diameter no greater than 6 Å, has to be influenced by two factors: the strength of the acid site bonding pyridine and the diffusion coefficient. During pyridine desorption from zeolites with secondary mesoporous channel system, diffusion coefficient should increase along with increase of the channel diameter and mesopores volume. The influence of the altered acid strength can be ruled out, because the experiments of carbon monoxide adsorption (static experiment) clearly demonstrated that the acid strength of Si–OH–Al groups did not changed with desilication. Similar results were observed in the experiments of CO adsorption and pyridine desorption from the zeolites of different channel connectivity [29].

The calculated concentrations of the Brønsted and Lewis centres are presented in Table 2. For both series of zeolites the number of Brønsted acid centres (calculated as the number of PyH^+ cations) is virtually independent of the desilication progress (differences below 20% which may be also attributed to the partial amorphization), while the number of Lewis centres increases drastically (by more than 100% in some cases). Such steep increase of the amount of Lewis acid sites may be the proof for the formation of the amorphous phase for zeolites treated with the most concentrated (1.0 M) base.

The fact that the number of Brønsted acid centres stays at the same level for non-treated and desilicated zeolites, while the intensity of the band characteristic of Si-OH-Al groups is decreasing seems to be a contradiction. This apparent inconsistency can be explained after analyzing the changes of the IR bands of PyH^+ and OH groups during pyridine thermodesorption.

Fig. 7 shows the IR maxima characteristic of OH groups in ZSM-5 and ZSM-12 zeolites treated in 0.1 M NaOH during pyridine desorption (for other zeolites the results were analogous, spectra not shown). Pyridine reacts with acidic OH groups in zeolites according to the scheme: zeol-OH + Py ↔ zeol-O^- + PyH^+. Pyridine desorption results in the decomposition of PyH^+ cations leading to the restoration of OH groups. For the case of desilicated zeolites, it can be easily observed that pyridine desorption at increasing temperatures, even if causing the decomposition of pyridinium cations (decrease of the 1545 cm^{-1} band) is not followed by the increase in the intensity of the band characteristic of OH groups. Therefore, in the examined zeolites some centres, able to protonate pyridine but at the same time not manifesting themselves as the band at ca. 3610 cm^{-1}, do exist. The possible nature and origin of such centres will be discussed later (*vide infra*).

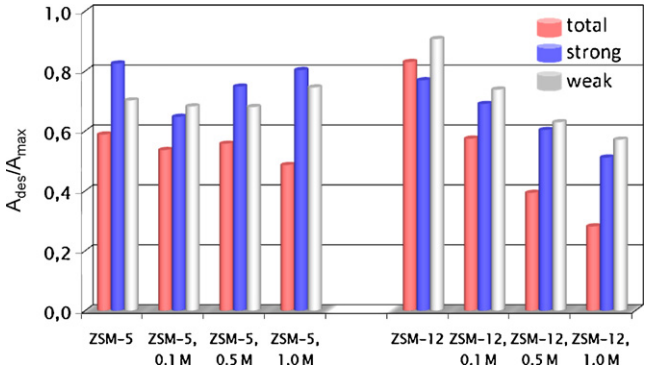

Fig. 8. Acid strength of OH groups in parent and desilicated zeolites ZSM-5 and ZSM-12. A_{des}/A_{max} represents a fraction of pyridinium ions (from the intensity of IR band at 1545 cm^{-1}) still present after desorption at given temperature (T_{des}).

The population of Brønsted acid sites can be therefore divided into two parts. The first is the population of the strong acid centres, Si–OH–Al groups. The second, is the population of weaker Brønsted centres, able to protonate pyridine but releasing it at lower temperatures than Si–OH–Al groups do. Concentration of both kinds of Brønsted centres can be estimated on the basis of pyridine thermodesorption experiment under assumption that almost all weak Brønsted centres released pyridine before this base started to desorb from the Si–OH–Al groups. This assumption obviously leads to some, although rather small, underestimation of the amount of weak Brønsted sites and overestimation of the strong Brønsted sites. As for all zeolites up to 450 °C the band characteristic of Si–OH–Al groups was not restored, this temperature was taken as a borderline. Intensity of the 1545 cm^{-1} pyridinium band was therefore taken as equal to the number of weak acid centres and the difference between the intensity of pyridinium band at 250 °C (maximal intensity) and 450 °C, was taken as the number of strong Brønsted sites: Si–OH–Al groups. It can be seen (Table 2) that although the overall concentration of the Brønsted sites is virtually constant, the concentration of the strong acid sites decreases and concentration of the weak acid centres increases. Therefore, the resultant average strength of acid centres should decrease with the desilication progress.

Usually the ratio of PyH^+ band intensities at 1545 cm^{-1} at different desorption temperatures A_{des}/A_{max} is taken as a determinant of the acid strength, where A_{des} is the intensity of the 1545 cm^{-1} band at the chosen desorption temperature, while A_{max} is the maximum intensity of this band – for all samples here – after desorption at 250 °C. The higher this ratio, the stronger are the Brønsted centres, because higher temperature is required to break the bond between the acidic OH group and pyridine molecule. In the case of series of desilicated zeolites discussed here two such ratios might be considered: separately for strong and weak Brønsted centres. If the same desorption temperature, 450 °C, is kept as borderline, the ratio A_{450}/A_{250} should characterize the strength of the weak Brønsted sites and the ratio A_{520}/A_{450} should represent the strength of the Si–OH–Al groups. The results of such comparison are visualized in Fig. 8. Now one can clearly observe that the acid strength of both types of zeolites is influenced in different way. While the strength of both strong and weak acid sites for zeolite ZSM-5 seems to be unaffected by the desilication, for ZSM-12 zeolite is decreasing steadily with the desilication progress (Fig. 8).

3.7. Origin of the weak Brønsted centres

Desilication resulted in the formation of mesopores, penetrating the zeolites' crystals and their framework. From the analysis of IR spectra it is obvious that more and more silanol groups

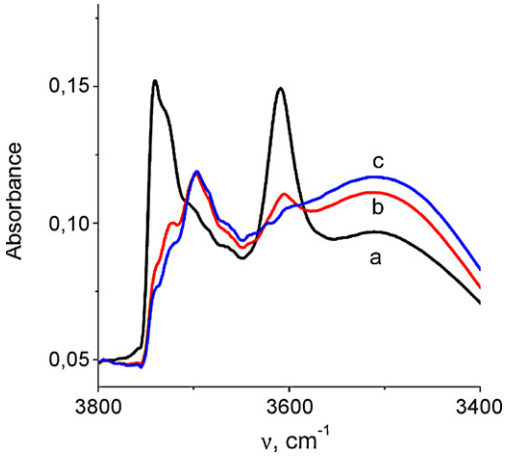

Fig. 9. IR spectra of OH groups in non-modified ZSM-5 zeolite interacting with α-pinene at 75 °C, a – activated zeolite, b – immediately after α-pinene adsorption, c – after 30 min contact.

emerged on the mesopores surface – they appeared when silanol nests, hydrogen-bonded silanols (vicinal SiOH) and siloxane or even Si–O–Al bridges were cut and fragments protruded into void of the mesopore. The dangling bonds had to be terminated and as a result Si–OH or both Si–OH and Al–OH groups (when Si–O–Al bridge was broken) appeared. It can be imagined that some of the mesopores were formed this way that Si–O–Al bond was not destroyed but as a whole situated on the mesopore's wall. Such Si–OH–Al group may be compared to the hydroxyls existing in mesoporous materials of M41S family [30] or of ITQ-2 material [31]. It is known that such OH groups are characterized by unusually low adsorption coefficient, therefore are practically invisible for IR spectroscopy [27]. What is more, their acid strength is also deeply lowered. All the features, characteristic for mesoporous Si–OH–Al groups can be attributed to the weak Brønsted sites, appearing as a result of desilication in both series of zeolites under investigation. Therefore we assume that Si–OH–Al groups protruding into the newly formed mesopores can be identified with Si–OH–Al groups analogous to the ones, formed in mesoporous materials. It is impossible to observe such OH groups in the IR spectra, as the weak acid centres constitute from 20 to 50% of all the Brønsted sites, and with greatly diminished absorption coefficient this maximum would be obscured by the IR band of standard bridging Si–OH–Al groups.

3.8. IR studies of α-pinene sorption

The diameter of α-pinene (6.8 Å × 6.9 Å) is clearly bigger than the channel diameter of both ZSM-5 (5.1 Å × 5.5 Å and 5.3 Å × 5.6 Å), and ZSM-12 (5.6 Å × 6.0 Å) zeolites. The question therefore arises whether some centres, present on unmodified sample were inaccessible to α-pinene and became accessible as a result of the mesopores formation. For that reason, α-pinene was adsorbed at the reaction temperature in zeolite of the smallest channels, i.e. ZSM-5. Recorded spectra are presented in Fig. 9. Under static conditions 30 min were enough for α-pinene to penetrate the whole zeolite crystal. The band of Si–OH–Al groups disappeared completely; therefore all OH groups were consumed by the reaction with pinene. It can be therefore concluded that even in unmodified zeolites all acid centres were accessible to α-pinene, thus formation of mesopores is responsible for the improved transport of reactants and not for the increased accessibility to centres, previously inaccessible.

Table 3
Catalytic performance of parent and desilicated zeolites ZSM-5 and ZSM-12. Sc – selectivity to camphene; Sl – selectivity to limonene; HRTP – high retention time products.

Sample	Conversion, mol%		Sc/Sc + Sl		HRTP	
	75 °C	90 °C	75 °C	90 °C	75 °C	90 °C
ZSM-5	11.4	10.0	49.5	49.3	3.3	6.7
ZSM-5, 0.1 M	9.3	9.5	45.5	46.2	3.2	3.6
ZSM-5, 0.5 M	17.1	17.2	50.3	53.7	4.1	3.0
ZSM-5, 1.0 M	29.9	27.5	49.8	49.8	3.1	3.4
ZSM-12	43.6	7.6	58.9	57.9	10.1	14.9
ZSM-12, 0.1 M	36.5	42.3	50.7	51.5	4.7	8.3
ZSM-12, 0.5 M	69.6	15.4	53.5	49.9	4.9	7.8
ZSM-12, 1.0 M	40.7	20.5	40.3	38.3	4.4	9.6

3.9. Catalytic study of α-pinene isomerization

Test reaction of α-pinene isomerisation was carried out at temperatures: 75 and 90 °C for 180 min in liquid phase. During reaction the catalyst, which was white initially, turned orange (75 °C) and brownish (90 °C). After the catalyst was removed from the solution, the intensity of the colour was diminished. The main products of α-pinene isomerisation are camphene, limonene, α-terpinene, *p*-cymene, terpinolene and fenchene together with HRTP (high retention time products), among them the oligomeric products with multiple bonds. The latter are appearing when the acid centres of high acid strength, enabling the successive reactions, are present [32]. Their quantity also increases with the increasing void space (presence of mesopores) and increased reaction temperature and lower conversion. Oligomers can be considered as coke precursors, effectively blocking the free reaction volume.

Catalytic activity of unmodified zeolite ZSM-12 is higher than ZSM-5 (Table 3) even if the concentration of acid centres is higher for the latter (Table 2). The most probable reason for higher activity of ZSM-12 in this case is the channel architecture. Although this zeolite is one-dimensional, the size of its 12-ring channels (5.6 Å × 6.0 Å) is bigger than those of ZSM-5 zeolite (10-rings: 5.1 Å × 5.5 Å and 5.3 Å × 5.6 Å), enabling not only faster diffusion of reactants but also easier formation of the bulky transition-state. On the other hand, in ZSM-12 zeolite selectivity to HRTP reaches almost 15% at 90 °C, thus suppressing the catalytic activity.

The influence of desilication on catalytic activity is best compared at 75 °C, temperature at which the formation of heavy oligomers is hindered.

Desilication increases catalytic activity of the samples, which is resulting mainly from the increase of the external surface (including mesopores surface) thus improved reactant transfer. The best results were achieved over ZSM-5 zeolite. The conversion on unmodified sample was ca. 11 mol%, while desilication improved it three times (to 30 mol% for zeolite treated with 1.0 M NaOH). In more open zeolite ZSM-12 the improvement was only ~1.5 times for zeolite ZSM-12, desilicated with 0.5 NaOH but further increase of the base concentration lowered the catalytic activity. The latter effect can be explained taking into account XRD data, showing that the crystallinity of this sample dropped to ca. 40%.

The influence of desilication on the selectivity towards main products (at 75 °C): camphene and limonene is not changing considerably mainly because there seemed to be enough space for the formation of the transition state leading towards both products in unmodified zeolites. Only for the reaction carried at 90 °C, the contribution of the HRTP is decreasing with desilication. This effect may be the result of combining effects of the increased reaction volume and slightly decreased acid strength of desilicated zeolites.

On the other hand, virtually constant amount of the HRTP on desilicated zeolites, especially for ZSM-12, much lower than for non-treated samples may be considered as a proof that α-pinene

conversion is carried out not at the external surfaces of the zeolitic crystals but at the internal, acidic sites. To which extent given reaction proceeds on the external surface, or in the pore system, or even in a rim of the crystal is not known in details for most of the zeolite systems studied so far. The only exception is when a very large difference between the molecule diameter and the entrance to the channel system exists, which is not a case here. Generally, discussion on this problem was carried out by Gündüz et al. [18] and Dimitrova et al. [33]. Authors show that if the reaction proceeds on the internal strong Brønsted sites, the main products of α-pinene conversion are the isomerisation products, and disproportionation of terpinene and terpinolene. For that reason we can suppose that the increased accessibility of the internal acidic centres on which such reactions, leading to HRTP, are proceeding (despite increased external surface area) is responsible for the better catalytic performance of desilicated zeolites.

4. Conclusions

Textural properties for both ZSM-5 and ZSM-12 zeolites change along with the concentration of NaOH used for desilication; the main alteration being the increasing contribution of mesopores, formed at the expense of micropores. ^{29}Si and ^{27}Al MAS NMR studies have shown that in both cases only the treatment in 1 M NaOH caused meaningful decrease in the amount of tetrahedral Al but still without significant increase of octahedral Al. At the same time the NMR signals from the framework Si decreased by 20–40% depending on the zeolite. NMR data show also that ZSM-5 zeolite is more resistant to the destructive power of NaOH than ZSM-12.

Acidic properties of desilicated zeolites were investigated by the adsorption of pyridine and CO followed by IR spectroscopy and set against the activity in α-pinene conversion. For both series the number of Brønsted acid centres (calculated as the number of PyH^+ cations) is virtually independent of the desilication progress (differences below 20%), while the number of Lewis centres increases drastically (by more than 100% in some cases).

Pyridine thermodesorption experiments showed that the significant part of Brønsted-type acidity cannot be identified with Si–OH–Al groups characterized by the IR band at ca. 3610 cm^{-1}. It was suggested that some Si–OH–Al groups are now protruding to the mesopores. In general, the acidic properties of such OH groups can be compared to the hydroxyls existing in mesoporous materials of M41S family. Such interpretation has never been offered before. The conversion of α-pinene, in the case of our zeolites changes parallel with the changes in the eternal surface and the number of weakly acidic OH groups, which are located at the mesopores' surface. Desilication process affected pore structure, acidity and catalytic activity of the zeolites under study.

Acknowledgement

IR measurements were made in the frames of the grant from the Ministry of Science and Higher Education, Warsaw, Poland (project no. N N204 1987 33).

References

[1] Y. Bouizi, G. Majano, S. Mintova, V. Valtchev, J. Phys. Chem. 111 (2007) 4535.
[2] C.J.H. Jacobsen, C. Madsen, J. Houzvicka, I. Schmidt, A. Carlsson, J. Am. Chem. Soc. 122 (2000) 7116.
[3] M. Ogura, S. Shinomiya, J. Tateno, Y. Nara, E. Kikuchi, M. Matsukata, Chem. Lett. (2000) 882.
[4] S. Van Donk, A.H. Janssen, J.H. Bitter, K.P. De Jong, Catal. Rev. 45 (2003) 297.
[5] J. Čejka, S. Mintova, Catal. Rev. 49 (2007) 457.
[6] S. Mintova, J. Čejka, Stud. Surf. Sci. Catal. 168 (2007) 301.
[7] H. Hamdan, B. Sulikowski, J. Klinowski, J. Phys. Chem. 93 (1989) 35.
[8] B. Sulikowski, J. Datka, B. Gil, J. Ptaszyński, J. Klinowski, J. Phys. Chem. B 101 (1997) 6929.
[9] J.C. Groen, J.A. Moulijn, J. Pérez-Ramírez, Micropor. Mesopor. Mater. 87 (2005) 153.
[10] S. Abello, A. Bonilla, J. Pérez-Ramírez, Appl. Catal. A: Gen. 364 (2009) 191.
[11] M.S. Holm, M.K. Hansen, C.H. Christensen, Eur. J. Inorg. Chem. 9 (2009) 1194.
[12] S. Abello, J. Pérez-Ramírez, Phys. Chem. Chem. Phys. 11 (2009) 2959.
[13] A. Bonilla, D. Baudouin, J. Pérez-Ramírez, J. Catal. 265 (2009) 170.
[14] J.C. Groen, S. Abello, L.A. Villaescusa, J. Pérez-Ramírez, Micropor. Mesopor. Mater. 114 (2008) 93.
[15] J.C. Groen, T. Sano, J.A. Moulijn, J. Pérez-Ramírez, J. Catal. 251 (2007) 21.
[16] J.C. Groen, R. Caicedo-Realpe, S. Abelló, J. Pérez-Ramírez, Mater. Lett. 63 (2009) 1037.
[17] A. Berenguer-Murcia, A.J. Fletcher, J. Garcia-Martinez, D. Cazorla-Amoros, A. Linares-Solano, K.M. Thomas, J. Phys. Chem. B 107 (2003) 1012.
[18] G. Gündüz, R. Dimitrova, S. Yilmaz, L. Dimitrov, M. Spassova, J. Mol. Catal. A: Chem. 225 (2005) 253.
[19] M.S. Holm, S. Svelle, F. Joensen, P. Beato, C.H. Christensen, S. Bordiga, M. Bjørgen, Appl. Catal. A: Gen. 356 (2009) 23.
[20] T. Seki, S. Ikeda, M. Onaka, Micropor. Mesopor. Mater. 96 (2006) 121.
[21] A. Corma, C. Corell, J. Perez-Pariente, Zeolites 15 (1995) 2.
[22] Ł. Mokrzycki, B. Sulikowski, Z. Olejniczak, Catal. Lett. 127 (2009) 296.
[23] D. Barthomeuf, Mat. Chem. Phys. 17 (1987) 49.
[24] R. Rachwalik, Z. Olejniczak, B. Sulikowski, Catal. Today 114 (2006) 211.
[25] M. Trombetta, T. Armaroli, A.G. Alejandre, J.R. Solis, G. Busca, Appl. Catal. A: Gen. 192 (2000) 125.
[26] M. Trombetta, G. Busca, J. Catal. 187 (1999) 521.
[27] K. Góra-Marek, M. Derewinski, P. Sarv, J. Datka, Catal. Today 101 (2005) 131.
[28] G. Busca, Catal. Today 41 (1998) 191.
[29] N. Žilková, M. Bejblová, B. Gil, S.I. Zones, A. Burton, C.Y. Chen, Z. Musilová-Pavlačková, G. Košová, J. Čejka, J. Catal. 266 (2009) 79.
[30] A. Corma, V. Fornés, M.T. Navarro, J. Perez-Pariente, J. Catal. 148 (1994) 569.
[31] A. Corma, V. Fornés, J.M. Guil, S. Pergher, Th.L.M. Maesencand, J.G. Buglass, Micropor. Mesopor. Mater. 38 (2000) 301.
[32] R. Rachwalik, Z. Olejniczak, J. Jiao, J. Huang, M. Hunger, B. Sulikowski, J. Catal. 252 (2007) 161.
[33] R. Dimitrova, G. Gündüz, M. Spassova, J. Mol. Catal. A: Chem. 243 (2006) 17.